Table 2. Summary of CFD modelling for cardiac abnormalities

Clinical applications	Data and evidence	Potential clinical impact	Limitations and challenges	Ref.
To evaluate biomechanical factors in the atherosclerotic process.	3D spatial patterns of steady and pulsatile flows in the left coronary artery were simulated, using a finite volume method.	Hemodynamic variables, include flow velocity, pressure and shear stress of the left anterior descending coronary bifurcation site were calculated.	There are marked individual variations in vascular structure and hemodynamics.	[17,18]
Characteristics of coronary arteries is represented by accelerating flow with physiological pressure and flow wave and it play a vital role in its localization.	Using a 3D FEM with transient flow and moving boundaries to simulate pulsatile flow with physiological pressure and flow wave forms characteristic of the coronary arteries.	It focused on the WSS and circumferential strain (CS) dynamic behaviour in a compliant model of a coronary artery including the curvature of the bending artery and physiological radial wall motion.	Computational mesh density resulted in acceptable errors in WSS.	[19]
Study the behaviour of the arterial motion and mathematical patterns on the hemodynamics of coronary artery of a left anterior descending (LAD) and compare the scale of the disease before and after the treatment.	3D arterial segments were reconstructed at 10 phases of the cardiac cycle for both pre- and post-intervention based on the fusion of intravascular ultrasound (IVUS) and biplane angiographic images.	Study the left anterior descending coronary artery hemodynamics before and after angioplasty.	Assumed same flow rate-time data at the inlet to the arterial segment, ignored the branches effect in the imaged segments as the IVUS images were only available in main vessel.	[24]
To inspect the left coronary artery (LCA) tree of the 3D wall pressure gradient (WPG) in quantity.	A model LCA tree, based on averaged human data set extracted from angiographies was adopted. The WPG was calculated with 44,452 nodes and a validated numerical code.	Spatial WPG differentiation indicates that locally low values of this physical parameter probably correlate to atherosclerosis localization.	Simulation findings have not been validated with a chronic model of left coronary artery.	[36]
For patients with severe coronary artery disease bypass grafting surgery is an effective treatment	CFD is used for 3D coronary bypass models of the aorto-right coronary bypass and the aorta-left coronary bypass systems.	To alleviate or delay the occurrence of vein graft disease. Also dimensions of the aorta, saphenous vein and the coronary artery to simulate the actual configurations at surgery.	Omit low WSS region near heel region of the anastomosis domain, and high WSS in toe region of the domain, resulting it prone to intimal hyperplasia.	[26]
Exam the stent-induced regional geometry influence distributions of WSS with 3D coronary artery.	Compute WSS at several intervals during the cardiac cycle, time averaged WSS, and WSS gradients via conventional techniques.	Better understand the regional geometry obtained at once after stent implantation. Evaluate the effect of stented vessel to a higher risk of neointimal hyperplasia and then restenosis.	Simulation is not compared with a chronic model of coronary artery restenosis.	[37]
To study the association of plaque thickness with endothelial shear stress.	3D luminal model using CFD.	Study the relationship of hemodynamic parameters with plaque thickness in the critical coronary region.	Simulation findings have not been benchmarked with a chronic model.	[38]
Three patients affected by MI and 3 normal subjects were assessed on their throbbing blood flow patterns in the left ventricular.	Compute velocity and pressure fields for patient specific 2D geometries with the combination of non-invasive MRI and CFD.	Found some useful information on intra-LV flow patterns with heart diseases for the flow patterns and pressure drop in the LV chamber.	2-D model are limited. Study exclude the mitral valve motion in the LV flow processes. Limited 6 cases only.	[15]
Patients with intermediate coronary stenosis.	Quick computational time of myocardial fractional flow reserve (FFR).	Quick computer model in quantifying the functional significance of moderately obstructed coronary arteries.	Limited sample size. Only validated de novo lesions. Selection bias is likely.	[44]
Effect of Cardiac Motion on Aortic Valve Flow for Computational Simulations of the Thoracic Aorta.	Approved IRB database of patients with congenital cardiovascular disease who had clinically indicated cardiac MRI studies in Children's Hospital of Wisconsin.	More precise measurements of hemodynamic variables via cardiac motion in AoV blood flow that are associated with long-term morbidity for the thoracic aorta, such as TKE and WSS.	The images used were of relatively low-pixel resolution (~1.75 mm) and hence introduce noise in relatively stationary periods in cardiac cycle despite the smoothing algorithm.	[10]
WSS Estimation of Thoracic Aortic Aneurysm with CFD.	3D aneurysm model was reconstructed from the CT scan slices using MIMICS. The original CT image file format was DICOM	model can be tested for varying stresses that an artery may be subjected (to) in day to day life.	Findings are based on limited population (i.e., one particular case)	[13]
CFD and echocardiography method to simulate blood flow in the single right ventricle	Full-volume 3D and 2D echo image loops were acquired with a S5-1 transducer at > 60 frames per second.	Qualitative comparisons demonstrated good concordance between the CFD-simulated results and Echo measured values	suffers some spatial and temporal resolutions and muscles and values were smoothing out to optimize CFD modelling	[34]

In the normal left ventricle, blood flow characteristics were studied using MRI, work-energy and N-S equations. They found that the 2D results' dynamic and energy characteristics were comparable to a 3D model. Through numerical analysis based on MRI of cardiac motion, 3D blood flow in a human left ventricle was further studied during myocardial dilation, the formation, growth and decay of vortices were analysed with flow patterns on different diametric planes [8]. Numerical proof-of-concept method was developed to study blood flow field under the influence of direct phase-contrast PC-MRI measurements and fluid physics model, permitting both the accuracy of PC-MRI and the high spatial resolution of CFD. This approach allowed data from fractional or comprehensive quantities to be merged into an advanced CFD solver, to enhance the accuracy of the subsequent flow approximations. The authors claimed that this filtered approach could reduce scan time, increase spatial resolution, and/or filtering the noises of PC-MRI measurements [9].
Numerical methods were developed to evaluate the impact of cardiac motion on blood flow measurements through the aortic valve so as to determine its effect on patient-specific localized hemodynamics [10, 11]. A CFD model was developed to study the vortex formation pattern and flow reversals in single right ventricle (SRV) and their results were considered as promising [13]. Use of CFD modelling in cardiac abnormalities numerical simulations are listed in Table 2.

3.2 Atherosclerosis (Aneurysm and Stenosis)

Atherosclerosis is a predominant cardiovascular disease, where fatty material is accumulated in the intima (inner layer) of arteries that supplies fluid to brain, heart, other vital organs including lower extremities [40]. An abnormal swelling of an artery due to the weakness in the arterial wall is termed as aneurysm; this could affect varieties of artery including the peripheral arteries and aorta. Book titled "Biomechanics and Mechanobiology of Aneurysms" covers the clinical context of aneurysm and CFD technique of endovascular repair of abdominal aortic aneurysms (AAA). These AAAs are irreversible dilation of infrarenal aorta which if untreated could grow and rupture [45]. The review article on 'Computational Biomechanics in Thoracic Aortic Dissection (AOD)' discussed about the importance of using CFD and their study to help doctors in improving their decision–making process in two types of Aortic disorders such as Type A (ascending aorta) and Type B (descending aorta)[46]. Computational techniques had been used to assess the movement of pulsatile displacement forces acting on thoracic Aortic endografts (Fig 4 and 5) and the study enhanced the understanding of power and relative position of the loads experiences in-vivo by thoracic aortic endografts to improve their design and performance [40].

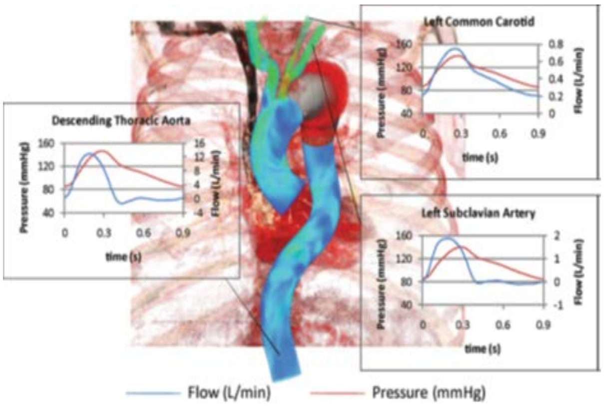

Fig.4: Flow and pressure waveforms in selected vessels obtained in the CFD analysis of a proximal descending thoracic aortic aneurysm (TAA) model. Note the physiologic range of the waveforms, presenting features such as retrograde flow in the descending aorta during early systole, and forward flow through the cycle in the common carotid artery. (This figure is reproduced with permission from Figueroa, C.A., Taylor, C.A., Chiou, A.J., Yeh, V., Zarins, C.K.: Magnitude and direction of pulsatile displacement forces acting on thoracic aortic endografts. J. Endovasc. Ther. 16(3), 350–358 (2009).

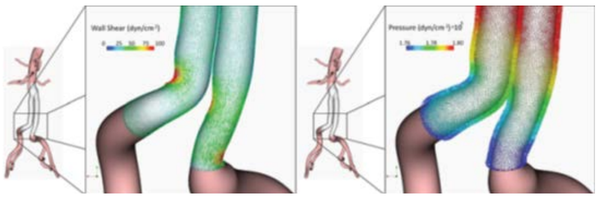
Fig.5: Wall shear (left) and pressure (right) stresses representing the actions of the blood on the endograft. These stresses are integrated over the surface of the endograft to calculate the total 3D force exerted by the pulsatile flow. Note that the pressure is several orders of magnitude

larger than the shear stress. Reproduced from Figueroa et al,[5].

The pathogenesis of AAA is multi-factorial and their development results in highly rated stresses and disturbed hemodynamic [30]. A CFD modelling paper presented the differences between healthy and the diseased cases mainly in the presence of highly raised up wall stresses and aggressive flow disturbances [47]. A study revealed a link or association between the AAA geometric parameters, abdominal flow patterns, wall stress shear (WSS), intraluminal thrombus (ILT), and AAA arterial wall rupture with CFD [29]. Appropriate viscosity models can be selected to compute non-Newtonian fluids and to solve fluid flow equation to obtain desired results. According to Fig 6 (a and b), the WSS, velocity and pressure of fluid flow can be visualised to predict the reason and identify the best method of intervention for atherosclerosis.

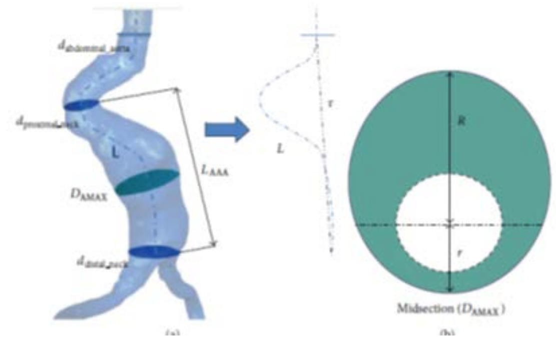

Fig.6: (a) Main geometrical parameters: LAAA aneurysm length, DMAX maximum diameter of the aneurysm$d$proximal neck beginning of the AAA sac, $d$distal neck ending of the AAA sac, $d$abdominal aorta nondeformed abdominal aorta diameter, L is the absolute length of the tortuous vessel, and τ is the imaginary straight line. (b) Schematic visualization of a cross-sectional AAA section, where r and R are defined as the radii measured at the midsection of the AAA sac from the longitudinal z-axis to the posterior and anterior walls.

A detailed study was made on the effects of a periodically excited wall on the oscillatory nature of flow structures and WSS [21-23]. Recent study was conducted on CFD analysis of a saccular shaped aneurysm, that resulted in marking the pulsatile blood flow as laminar is correct and WSS values did not go over the prediction. Using magnetic resonance imaging, Yim et al, (2004) put forth a methodology for the calculation of renal artery differential pressure (RADP). Convincing CFD models were built from magnetic resonance (MR) angiography and phase-contrast [48].

Preliminary study was done on hyper dynamic analysis of renal artery stenosis (RAS), using CFD technique based on non-improved steady-state free slow-moving magnetic resonance angiography. Their study showed that non-improved-MRA-based CFD could be used to unsystematically assess hemodynamic measurable factors of RAS, and the obtained variables would yield useful details related to stratification of the stenosis and more therapeutic treatment [49]. The effect of the renal artery ostium flow diverter on hemodynamic and atherogenesis was investigated using CFD modelling techniques [50].

The effects of spiral form of flow on hemodynamic changes in aorta-renal bifurcations were studied and the results showed that the spirality effects causes an evident variation in blood velocity distribution by creating only slight changes in fluid shear stress patterns, and indicated that spiral nature of blood flow has atheroprotective effects in renal arteries and hence to be considered in the analysis of aorta and renal arteries [32]. To study the behaviours of tracers flowing through the kidney CFD compartmental modelling was used to validate its accuracy [51].

3.3 Ophthalmology

Usage of CFD in ophthalmology studies have been increased in recent years. For minimizing inaccuracies researchers while developing retinal mathematical models always try to construct the model that best resemble the actual system [52]. An article published in the American Academy of Ophthalmology website gives a brief summary of CFD use in ophthalmological diseases [53]. The process which damages the optic nerve by increasing the intraocular pressure and blocking the outflow is called Glaucoma, there are lot of complex question regarding the brittle balance between the inflow and the outflow of aqueous humour in normal human eye which is yet to be completely understood [54]. It was mentioned by Sultan et al, that the IOP (intraocular pressure) though excluded from the glaucoma definition remains as a casual risk factor [55]. IOP is related with increased resistance to aqueous humour outflow and it is not different from normal (nonglaucomatous individual and these remarks have led to a better understanding of the aqueous humour properties and the support of CFD. Many researchers have tried to demonstrate the elements of aqueous humour outflow with reference to different parameters of the human eye in the anterior chamber [56-59]. A Newtonian fluid was modelled for the aqueous humour and a linear elastic solid for the iris and it was to compute the iris contour in the eyes.

Ooi and Ng (2008) developed a 2-D model of human eye to understand the presence of natural flow of aqueous humour and to investigate the flow effects inside the anterior chamber [60]. In Ooi et al, (2011) using the above model research was conducted to learn about the natural convection in the anterior chamber on the ocular heat transfer as shown in Fig 7. CFD is used to investigate the crystalline lenses and ciliary body structures. John et al, (1996) defined lens as a clear biconvex form in the eyes that in co–occurrence with the cornea helps to refract light that needs to be focused on the retina, lens is used to change the focal distance of the eye so it can correctly focus on objects to indulge various focal length distances. For analysing catalase activities, lens epithelial samples were taken, and analysts tried to apply CFD to stimulate heat and its exposure caused damage to lens. Sharon et al 2008 led analyst group showed that bakery heat exposure can cause damage to the eye lens depending on its length of the exposure [58]. Heys et al, (2003) stated that through tremendous effort they were able to include computational assessment in the role of accommodation in pigmentary glaucoma.

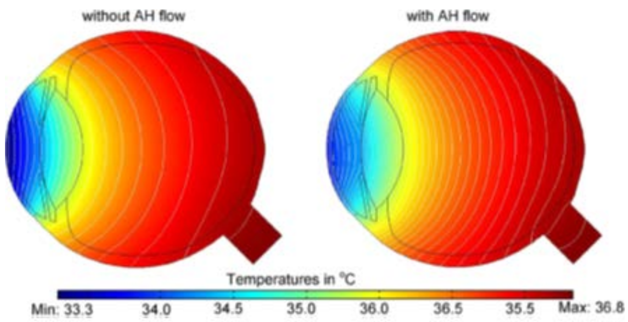

Fig.7: A typical temperature distribution of the eye with and without AH flow in the vertical orientation. (This figure is reproduced from - Simulation of aqueous humour hydrodynamics in human eye heat transfer, EH Ooi, EYK Ng, Computers in Biology and Medicine 38 (2008) 252 – 262).

3.4 Fluid and Air Flow in Lungs

Incompressible flow equation by Navier-Stokes well predicts the air flow through lungs at low speeds [61]. CFD plays as a powerful tool to predict the transport and deposition of gases and particles in the respiratory tract system. It is limited to relatively small regions due to the complexity of airways at respiratory path. Numerous studies were carried out to simulate the lungs with CFD approach. The process needs an accurate CAD model using MRI and CT scans to generate mesh model for the geometry [62]. This helps physicians to develop medical devices and necessary treatments methods.

A study on numerical simulation to visualize the flow characteristics in an empty Rochester style inhalation chamber during steady-state and transient pollutant concentrations was employed with commercial CFD program [63]. To evaluate the turbulent effects, polydisperse aerosol size distribution, and multiple lung lobes deposition in the mouth–throat (MT) and entire tracheobronchial (TB) airways, a new CFD approach was established [63, 64]. The authors developed CFD modelling of the stochastic individual pathway (SIP) to simulate the transport and deposition of whole lung aerosols. This CFD approach simulates the upper airways through the lobar bronchi using characteristic models derived from Computed Tomography (CT) scan images. These models are also rapidly prototyped for generating corresponding in-vitro deposition data. SIP approach also simulates the transport and deposition in the remainder of the tuberculosis (TB) airways which ensembles to create and compute individual pathways. Several recent studies from this group provide detailed in-vitro deposition data from realistic inhalers using characteristic models of MT, nasal airways and upper TB region [64, 65]. Very good agreement was achieved between the in-vitro deposition data and CFD predictions for pharmaceutical aerosols based on numerical model refinements implemented through user-defined functions (UDFs). The SIP approach was found to be a reliable method for simulating lung deposition of pharmaceutical aerosols with a computational multiple order of magnitude compared with simulating all the tracheobronchial airways.

An investigation on patient-specific respiratory pathway under physiological boundary conditions using a CFD model of a healthy, a stenotic and a post-operatory stented human trachea estimated outflow pressure waveforms which allows the computation of peripheral impedance of truncated bronchial generation and modelling the lungs as fractal networks [66]. Recently, a CFD transient simulation of the cough clearance process was analysed with Eulerian wall film model [67]. In this research, a methodology was proposed to predict cough mucus clearance which successfully enabled the simulation and quantification of the overall performance of cough. Researchers proved that CFD can be used to model and predict fluid and air flow in lungs which are considered clinically as very complex.

3.5 Cerebrospinal Fluid Flow

Brain, blood and cerebrospinal fluid (CSF) co-exist and preserve a constant volume in intracranial space. The role of CSF is very crucial as it protects the brain from injury and delivers nutrients to and from the brain along with the removal of waste products. CSF dynamics in the cervical spinal subarachnoid space (SSS) are useful to help diagnose and assess craniospinal disorders like Chiari malformation [68]. CSF fluctuation is a complex phenomenon in fluid dynamics as it flows inside the craniospinal cavities in a pulsatile manner which results from the systolic expansion and contraction of cerebral blood vessels. Clinically, it is still unclear the complex multifactorial processes of the development, progression, and rupture of cerebral aneurysms. In recent years, many researchers have focused on brain aneurysm research. Contributions were made using patient-specific CFD models for brain aneurysm and highlighted the mechanisms of computational models for patient-specific assessment on brain aneurysm rupture risk and patient management [68]. It is also clinically accepted that hemodynamics plays a major role in brain aneurysm. However, there is no consensus among researchers and clinicians on implication of any hemodynamic variable in these mechanisms. Hemodynamics strongly depends on the vascular geometry and it requires investigations to better understand the interaction between mechano-biological wall responses and hemodynamic loading. These govern the natural history of cerebral aneurysms and it is needed to study well on the in-vivo aneurysmal hemodynamic environment [69]. CFD simulations and in-vitro flow models are based on 2D phase contrast (PC) MRI measurements and additional anatomical data. These models and simulations allow non-invasive analysis of the CSF flow environment in healthy and patient cases [70-72]. However, it is difficult to quantify 3D complexities using the unidirectional encoding 2D phase contrast MRI CSF flow measurements within the CSF flow field.

CFD studies of CSF flow in the cervical spine have been conducted under geometrically simplified subject-specific 3D models without fine anatomical structures and with idealized spinal cord nerve rootlets and denticulate ligaments [68-72].

Yiallourou et al (2012) used time-resolved 3D velocity encoded phase-contrast MRI (4D PC MRI) in 3 healthy volunteers and 4 CM patients and compared the 4D PC MRI measurements to subject-specific 3D CFD computations [72]. They considered rigid-walled geometry and didn’t include small anatomical structures like denticulate ligaments, nerve roots and arachnoid trabeculae. They then 4D PC MRI flow measurements and T2-weighted anatomy MRI images at the cervical-medullary junction of a single healthy volunteer and obtained CFD simulations considering the fluid to be incompressible and Newtonian. These results support the use of CFD modelling in CSF flow for subject specific MRI within the cervical spine also provide consistent quantitative geometric and hydrodynamic parameters to potential clinical diagnostic and assessment purposes.

3.6 Artificial Organ Design

Artificial organs are engineered devices that are implanted or integrated into human body to replace non-functional natural organ and helps patient to return to normal life. Prototype development stage of artificial organs involves many numerical simulations on hemodynamics with optimal geometry to make devices clinically viable. Simulated flow permit information on the size and location of stagnation zones and thus the local shear rate. These parameters can be used to correlate to the extent of thrombus formation and haemolysis which are important to establish the success of a blood pump [73]. Ventricular assist devices (VADs) are mechanical pumps to augment or replace the function of one or more chambers of failing heart. Satisfactorily blood damage models are lacking in numerical analysis of VADs despite much efforts, that limit the full potential of CFD. Implantable VADs have been regarded as a promising instrument in the clinical treatment of patients with severe heart failures. Chua et al. 2006, illustrated, a 3D model of the Kyoto-NTN magnetically suspended centrifugal blood pump and provide CFD solution of the inner flow field of the pump including the velocity profiles, static pressure distributions and the shear stress distributions of the blood [74].

Katharine et al. (2011) reviewed the use of CFD in the development of VADs and listed state-of-the-art CFD analysis of blood pumps, with a practical critical review of the studies. Also, the paper presented a summary of blood damage models and their difficulties in CFD implementation, explained the gaps in knowledge with future work [75]. Farag et al. (2014) published a review article presenting results on patients receiving mechanical assist devices using CFD simulations for end-stage heart failure [76].

The use of CFD extends in evaluating the performance of artificial organs such as to predict the physiological behaviour of a prosthetic heart valve. Claudio Capelli et al. (2017) investigated the differences in hemodynamic performances using different anchoring systems with the help of CFD analysis [77]. They adopted a combined approach of commercially available experimental and computational tools for bio-prosthetic aortic valves. Numerical computations allow identification of useful information on the locations of high shear rates in the flow which damage the blood cells and needs proper boundary conditions. The use of CFD technique is being consistently extended for many other biomedical applications like vocal tract analysis, nose and sinus flows, joint lubrication, spinal fluid flows etc. In addition to these biomedical applications, the use of CFD is also employed in developing medical devices for surgical procedures.

4 Summary

With the advancement of high-speed computers and newer generation computational software, CFD has been a more economical and feasible alternative high-end technology-based tool to diagnose and predict circulatory abnormalities. Biomedical engineering researchers now could gain knowledge on flow behaviour of body fluids and understand how the system components are expected to perform. Thus, it makes possibilities to improve bio-fluid physiology studies and to better designed medical treatments and devices. Computational modelling tools provide an opportunity to evaluate multiple situations for an extremely difficult condition to setup experimental system. Several laboratories work on numerical modelling of human circulatory system for improving abnormality risk-prediction. The usage of CFD is being consistently stretched for many biomedical applications including nose and sinus flows, vocal tract analysis, joint lubrication, spinal fluid flows etc. Apart from the above applications, computational techniques are also applied in developing medical devices in surgical procedures. The reducing cost of computational time, memory and development of improved mathematical models, biomedical applications are further expected in extending the implementation of versatile CFD techniques and allow in saving human lives. In near future, it would be possible for a physician to compile CT of a patient with digital captured computational model. The properties and boundary conditions would be enforced, and the physician can visually see the flow phenomenon simulated inside. Moreover, this can be integrated with a bio 3D printer to tailor-make prosthesis like heart valves, stents, etc., based on the CT and computational results, ensuring that it is patient specific and with an in-built fail-safe mechanism. Overall, this review adequately describes the detail of state-of-the-art in terms of “horizontal” technology (CFD) or provide sufficient detail to understand the implications of application of the technology to specific “vertical” biomedical problems. In coming years use of CFD in biomedical and its related field is likely to surge.

Nomenclature
c Specific heat capacity [J/kg. ^{o}C]
h Heat transfer coefficient [W/m^{2} ^{o}C]
k Thermal conductivity [W/m^{2} ^{o}C]
L length [m]
q Volumetric heat generation [W/m^{3}]
T Temperature [^{o}C]
w Blood perfusion rate [kg/(s.m^{3})]
Subscripts: a- Artery, b- Blood, e- Environment, m- Metabolic

References:

[1] Pennes H H, Analysis of Tissue and Arterial Blood Temperatures in the Resting Human Forearm, *Journal of Applied Physiology*, Vol.1, 1948, pp. 93–122.

[2] Joseph Feher, Quantitative Human Physiology: An Introduction. Academic Press Series in Biomedical Engineering, Academic Press, 2012.

[3] Michael Chappell, Stephen Payne, *Physiology for Engineers: Applying Engineering Methods to Physiological Systems*, Springer, 2015.

[4] Wendt, John (Ed.), *Computational Fluid Dynamics: An Introduction*, Springer International Publishing, 2009.

[5] Kajishima, Takeo, Taira, Kunihiko, *Computational Fluid Dynamics: Incompressible Turbulent Flows*, Springer International Publishing, 2017

[6] Joel H. Ferziger, Milovan Peric, *Computational Methods for Fluid Dynamics*, Springer International Publishing, 2002.

[7] Khalafvand SS, Ng EY-K, Zhong L, Hung TK, Three-dimensional diastolic blood flow in the left ventricle, *Journal of Biomechanics*, Vol. 50, No. 1, pp. 71–76 (in-press).

[8] TK Hung, Khalafvand, S.S., Ng, E. Y-K, Fluid Dynamic Characteristics of Systolic Blood Flow of the Left Ventricle, *Journal of Mechanics in Medicine and Biology*, Vol. 15, No. 1, 2015, pp. 1550047-1 - 1550047-20.

[9] Vinicius C. Rispoli, Jon F. Nielsen, Krishna S. Nayak and Joao L. A. Carvalho, Computational Fluid Dynamics Simulations of Blood Flow Regularized by 3D Phase Contrast MRI, *Biomedical Engineering Online*, Vol.14, 2015, pp.110

[10] Wendell DC, Samyn MM, Cava JR, Krolikowski MM, LaDisa JF Jr, The Impact of Cardiac Motion on Aortic Valve Flow Used in Computational Simulations of the Thoracic Aorta, *Journal of Biomechanical Engineering*, Vol. 138, No. 9, 2016, pp. 09010011-090100111.

[11] Lee BK, Computational Fluid Dynamics in Cardiovascular Disease, *Korean Circulation Journal*, Vol. 41, 2011, pp.423–430.

[12] Krishna Sriram, Marcos Intaglietta, Daniel M. Tartakovsky, Non-Newtonian Flow of Blood in Arterioles: Consequences for Wall Shear Stress Measurements, *Microcirculation*, Vol. 21, No. 7, 2014, pp. 628–639.

[13] Febina J, Mohamed Yacin Sikkandar, Sudharsan N M, Wall Shear Stress Estimation of Thoracic Aortic Aneurysm Using Computational Fluid Dynamics, *Computational and Mathematical Methods in Medicine*, Vol. 2018, Article ID 7126532, 2018, pp.12 pages.

[14] Sudharsan NM, Ng EYK, Teh SL, Surface Temperature Distribution of a Breast With and Without Tumour, *Computer Methods in Biomechanics and Biomedical Engineering*, Vol. 2, No.3, 1998, pp.187 – 199.

[15] Khalafvand SS, Ng EYK, Zhong L, CFD Simulation of Flow Through Heart: A Perspective Review, *Computer Methods in Biomechanics and Biomedical Engineering*, Vol. 14, No. 1, 2011, pp.113-132.

[16] Mehul Patel, 7 Stages of a Typical CFD Simulation, *Engineering Exchange*, 2017.

[17] Lee BK, Kwon HM, Kim D, Yoon YW, Seo JK, Kim IJ, Roh HW, Suh SH, Yoo SS, Kim HS, Computed Numerical Analysis of the Biomechanical Effects on Coronary Atherogenesis Using Human Hemodynamic and Dimensional Variables, *Yonsei Medical Journal*, Vol. 39, 1998, pp. 166-74.

[18] Lee BK, Lee JY, Hong BK, Park BE, Kim DS, Kim DY, Cho YH, Yoon SJ, Yoon YW, Kwon HM, Roh HW, Kim I, Park HW, Han SM, Cho MT, Suh SH, Kim HS, Hemodynamic Analysis of Coronary Circulation in Angulated Coronary Stenosis Following Stenting, *Yonsei Medical Journal*, Vol. 43, 2002, pp. 590-600.

[19] Qiu Y, Tarbell JM, Numerical Simulation of Pulsatile Flow in a Compliant Curved Tube Model of a Coronary Artery, *Journal of Biomechanical Engineering*, Vol. 122, 2000, pp.77-85.

[20] Siauw W.L., Ng, E. Y-K, Mazumdar J, Unsteady Flow of Fluids Through Arterial Stenosis: A Comparative Study of Non-Newtonian Models With Operator Splitting Scheme, *Journal of Medical Engineering & Physics*, Vol. 22, 2000, pp. 265 - 277.

[21] Ng, E. Y-K, Siauw W.L, Unsteady Viscous Flow Model on Moving Domain through Stenotic Artery, *International Journal of Engineering in Medicine*, Vol. 215, No. 2, 2001, pp. 237 – 249.

[22] Ng, E. YK, Siauw WL, Chong CK, Simulation of Oscillatory Wall Shear Stress in Channel with Moving Indentation,

International Journal for Numerical Methods in Engineering, Vol. 54. No. 10, 2002, pp. 1477-1500.

[23] Ng, E. Y-K, Siauw, W.L, Modelling of Fluid-wall Interactions for Viscous Flow in Stenotic Elastic Artery, *Progress in Computational Fluid Dynamics: An International Journal*, Vol. 2, No. 1, 2002, pp. 33 – 44.

[24] Ramaswamy SD, Vigmostad SC, Wahle A, Lai YG, Olszewski ME, Braddy KC, Brennan TM, Rossen JD, Sonka M, Chandran KB, Fluid Dynamic Analysis in a Human Left Anterior Descending Coronary Artery With Arterial Motion, *Annals of Biomedical Engineering*, 32, 2002, pp.1628-1641.

[25] Giannoglou GD, Soulis JV, Farmakis TM, Giannakoulas GA, Parcharidis GE, Louridas GE, Wall Pressure Gradient in Normal Left Coronary Artery Tree, *Medical Engineering Physics*, 27, 2005, pp. 455-64.

[26] Sankaranarayanan M, Chua LP, Ghista DN, Tan YS, Computational Model of Blood Flow in the Aorto-Coronary Bypass Graft, *Biomedical Engineering Online*, Vol. 4, 2005, pp.14.

[27] Marsden AL, Bernstein AJ, Reddy VM, Shadden SC, Spilker RL, Chan FP, Taylor CA, Feinstein JA, Evaluation of a Novel Y-shaped Extracardiac Fontan Baffle Using Computational Fluid Dynamics, *The Journal of Thoracic and Cardiovascular Surgery*, Vol. 137, No. 2, 2009, pp.394-403

[28] Khalafvand, S.S., Ng, E. Y-K., L. Zhong, T.K. Hung, Fluid-dynamics Modeling of the Human Left Ventricle With Dynamic Mesh for Normal and Myocardial Infarction: Preliminary Study, *Computers in Biology and Medicine*, Vol. 42, No.8, 2012, pp. 863-870.

[29] Eduardo Soudah, E.Y.K. Ng, T.H. Loong, Maurizio Bordone, Uei Pua, Narayanan Sriram, CFD Modelling of Abdominal Aortic Aneurysm on Hemodynamic Loads Using a Realistic Geometry with CT, *Computational and Mathematical Methods in Medicine*, Vol. 2013, Article ID 472564, 2013, pp. 9.

[30] Gasser TC, Nchimi A, Swedenborg J, Roy J, Sakalihasan N, Böckler D, Hyhlik-Dürr A, A Novel Strategy to Translate the Biomechanical Rupture Risk of Abdominal Aortic Aneurysms to their Equivalent Diameter Risk: Method and Retrospective Validation, *European Journal of Vascular and Endovascular Surgery*, Vol. 47, No. 3, 2014, pp.288–95.

[31] Dalasm, N. K. H, Longest, P. W, Deposition of Particles in the Alveolar Airways: Inhalation and Breath-Hold With Pharmaceutical aerosols, *Journal of Aerosol Science*, Vol. 79, 2015,pp. 15-30

[32] Javadzadegan A, Simmons A, Barber T, Spiral Blood flow in aorta-renal bifurcation models, Comput Methods Biomech Biomed Eng. 19 (9):, 2016, pp. 964-76

[33] Caruso MV, Serra R, Perri P, Buffone G, Calio FG, DE Franciscis S, Fragomeni F, Evaluation of Sedentary Lifestyle Effects on Carotid Hemodynamics and Atherosclerotic Events Incidence, *Acta of Bioengineering and Biomechanics*, Vol.19, No.3, 2017, pp. 42-52.

[34] Li-Jun Chen, Zhi-Rong Tong, Qian Wang, Yu-Qi Zhang, Jin-Long Liu, Feasibility of Computational Fluid Dynamics for Evaluating the Intraventricular Hemodynamics in Single Right Ventricle Based on Echocardiographic Images, *BioMedical Research International*, Vol. 2018, Article ID 1042038, 2018, pp.11.

[35] Hao Liu, Fuyou Liang, Jasmin Wong, Takashi Fujiwara, Wenjing Ye, Keniti Tsubota Michiko Sugawara, Multi-scale Modeling of Hemodynamic in the Cardiovascular System, *Acta Mechanica Sinica*, Vol. 31, No. 4, 2015, pp. 446–464.

[36] Giannoglou GD, Soulis JV, Farmakis TM, Giannakoulas GA, Parcharidis GE, Louridas GE, Wall Pressure Gradient in Normal Left Coronary Artery Tree, *Medical Engineering Physics*, Vol. 27, 2005, pp. 455-64.

[37] LaDisa JF Jr, Olson LE, Douglas HA, Warltier DO, Kersten JR, Pagel PS, Alterations in Regional Vascular Geometry Produced by Theoretical Stent Implantation Influence Distributions of Wall Shear Stress: Analysis of a Curved Coronary Artery Using 3D Computational Fluid Dynamics Modeling, *Biomedical Engineering Online*, Vol. 16, 2006, pp. 40.

[38] Papafaklis MI, Bourantas CV, Theodorakis PE, Katsouras CS, Fotiadis DI, Michalis LK, Association of Endothelial Shear Stress With Plaque Thickness in a Real Three-Dimensional Left Main Coronary Artery Bifurcation Model, *International Journal of Cardiology*, Vol. 115, 2007, pp. 276-278.

[39] Marsden AL, Bernstein AJ, Reddy VM, Shadden SC, Spilker RL, Chan FP, Taylor CA, Feinstein JA, Evaluation of a Novel Y-shaped Extracardiac Fontan Baffle Using Computational Fluid Dynamics, *The Journal of Thoracic and Cardiovascular Surgery*, Vol. 137, No. 2, 2009, pp. 394-403

[40] Taylor CA, Figueroa CA, Patient-Specific Modeling of Cardiovascular Mechanics, *Annual Review of Biomedical Engineering*, Vol. 11, 2009, pp. 109–34.

[41] Samady H, Eshtehardi P, McDanie MC, Suo J, Dhawan SS, Maynard C, Timmins LH, Quyyumi AA, Giddens DP, Coronary Artery Wall Shear Stress is Associated With Progression and Transformation of Atherosclerotic Plaque and Arterial Remodeling in Patients With Coronary Artery Disease, *Circulation*, Vol. 124, No. 7, 2011, pp. 779-88. .

[42] Khalafvand, SS, Zhong L, Ng EYK, Three-Dimensional CFD/MRI Modeling Reveals That Ventricular Surgical Restoration Improves Ventricular Function by Modifying Intraventricular Blood Flow, *International Journal for Numerical Methods in Biomedical Engineering*, Vol. 30, No.10, 2014, 1044-1056.

[43] Khalafvand SS, Hung T-K, Ng EY-K, Zhong L, Kinematic, Dynamic and Energy Characteristics of Diastolic Flow in the Left Ventricle, *Computational and Mathematical Methods in Medicine*, Article ID 701945, 2015, pp. 12 pages.

[44] Tu J, Yeoh GH, Liu C, *Computational Fluid dynamics. A Practical Approach*, Elsevier Publishers, 2008.

[45] McGloughlin, *Biomechanics and Mechanobiology of Aneurysms*, Springer Publishers, 2011.

[46] Doyle B J, Norman P E, Computational Biomechanics in Thoracic Aortic Dissection: Today's Approaches and Tomorrow's Opportunities, *Annals of Biomedical Engineering*, 2016, Vol. 44, No. 1, pp. 71-83.

[47] Tejas Canchi, D. Kumar, Ng, E. Y.K., Narayanan Sriram, A Review of Computational Methods to Predict the Risk of Rupture of Abdominal Aortic Aneurysms, *BioMedical Research International*, Vol. 2015, Article ID 861627, 2015, pp. 12 pages.

[48] Yim PJ, Cebral JR, Weaver A, Lutz RJ, Soto O, Vasbinder GB, Ho VB, Choyke PL, Estimation of the Differential Pressure at Renal Artery Stenosis, *Magnetic Resonance in Medicine*, Vol. 51, No. 5, 2004, pp. 969-77.

[49] Zhang W, Qian Y, Lin J, Lv P, Karunanithi K, Zeng M, Hemodynamic Analysis of Renal Artery Stenosis Using Computational Fluid Dynamics Technology Based on Unenhanced Steady-State Free Precession Magnetic Resonance Angiography: Preliminary Result, *International Journal of Cardiovascular Imaging*, Vol. 30, No. 2, 2014, pp. 367-75.

[50] Scott Albert, Robert S Balaban, Edward B Neufeld, Jenn Stroud Rossmann, Influence of the Renal Artery Ostium Flow Diverter on Hemodynamic and Atherogenesis, *Journal of Biomechanics*, Vol. 47, No. 7, pp. 1594–1602.

[51] Suriyanto, Ng E YK, XJ Say, CE Ng David, YX Sean, SD Kumar, Quantitative Means for Differentiating Renal Obstruction by Analyzing Renography via Compartmental Modeling of Renal Fluid Flow Rate, *Nuclear Medicine Communications*, Vol. 37, No. 9, 2016, pp. 904–910.

[52] Fitt AD, Gonzalez G, Fluid Mechanics of the Human Eye: Aqueous Humour Flow in the Anterior Chamber, *Bulletin of Mathematical Biology*, Vol. 68 2006, pp. 53–71

[53] Konstantinos Tsaousis, Computational Fluid Dynamics (CFD) in Ophthalmology, *American Academy of Ophthalmology Website*, 2015.

[54] Kwon YH, Fingert JH, Kuehn MH, Alward WL, Primary Open-Angle Glaucoma, *The New England Journal of Medicine*, Vol. 360, 2009, pp.1113-24.

[55] Sultan MB, Mansberger SL, Lee PP, Understanding the Importance of IOP Variables in Glaucoma: A Systematic Review, *Survey of Ophthalmology*, Vol. 54, 2009, pp. 643-662.

[56] Schachar RA, The Mechanism of Accommodation and Presbyopia, *International Ophthalmology Clinics* , Vol. 46, 2006, pp. 39-61

[57] Jump up, Tamm ER, Fuchshofer R, What Increases OutflowRresistance in Primary Open-Angle Glaucom, *Survey of Ophthalmology*, Vol. 52, 2007, Suppl 2: S101-4.

[58] Sharon N, Bar-Yoseph PZ, Bormusov E, Dovrat A, Simulation of Heat Exposure and Damage to the Eye Lens in a Neighborhood, *Experimental Eye Research.*, Vol. 87, No. 1, pp.49-55.

[59] Kapnisis K, Doormaal MV, Ross Ethier C. Modeling Aqueous Humor Collection From the Human Eye, *Journal of Biomechanics*, Vol. 42, 2009, pp. 2454-7.

[60] Ooi EH, Ng E YK, Effects of Natural Convection Inside the Anterior Chamber on the Ocular Heat Transfer, *International Journal for Numerical Methods in Biomedical Engineering*, Vol. 27. No. 3, 2011, pp. 408-423.

[61] Nowak N, Kakade PP, Annapragada AV, Computational Fluid Dynamics Simulation of Airflow and Aerosol Deposition in Human Lungs, *Annals of Biomedical Engineering*, Vol. 31, No. 4, 2003, pp. 374-90.

[62] Geng Tian, P. Worth Longest, Development of a CFD Boundary Condition to Model Transient Vapor Absorption in the Respiratory Airways, *Journal of Biomechanical Engineering*, Vol. 132, No. 5, 2010, pp. 051003-051003.

[63] Longest, P. W., Tian, G., Walenga, R. L., Hindle, M, Comparing MDI and DPI Aerosol Deposition Using in Vitro Experiments and a New Stochastic Individual Path (SIP) Model of the Conducting Airways, *Pharmaceutical Research*, Vol. 29, 2012, pp. 1670-1688.

[64] Geng T, Longest W, Su G, Ross L Walenga, Hindle M, Development of a Stochastic Individual Path (SIP) Model for Predicting the Tracheobronchial Deposition of Pharmaceutical Aerosols: Effects of Transient Inhalation and Sampling the Airways, *Journal of Aerosol Science*, Vol. 42, No. 11, 2011, pp. 781-799.

[65] M. Malvè, S. Chandra, J. L. López-Villalobos, E. A. Finol, A. Ginel & M. Doblaré, CFD Analysis of the Human Airways Under Impedance-Based Boundary Conditions: Application to Healthy, Diseased and Stented Trachea, *Computer Methods in Biomechanics and Biomedical Engineering*, Vol. 16, No. 2, 2013, pp. 198-216.

[66] Concepción Paz, Eduardo Suárez & Jesús Vence, CFD Transient Simulation of the Cough Clearance Process Using an Eulerian Wall Film Model, *Computer Methods in Biomechanics and Biomedical Engineering*, Vol. 20, No. 2, 2017, pp. 142-152.

[67] Clarke EC, Fletcher DF, Stoodley MA, Bilston LE, Computational Fluid Dynamics Modelling of Cerebrospinal Fluid Pressure in Chiari Malformation and Syringomyelia, *Journal of Biomechanics*, Vol. 46, No. 11, 2013, pp. 1801-9.

[68] Daniel M. Sforza1, Christopher M. Putman, Juan R. Cebral, Computational Fluid Dynamics in Brain Aneurysms, *International Journal for Numerical Method Biomedical Engineering*, Vol. 28, 2012, pp. 801–808.

[69] Sweetman B, Linninger AA, Cerebrospinal Fluid Flow Dynamics in the Central Nervous System, *Annals of Biomedical Engineering*, Vol. 39, 2011, pp. 484-496.

[70] Hsu Y, Hettiarachchi HD, Zhu DC, Linninger AA, The Frequency and Magnitude of Cerebrospinal Fluid Pulsations Influence Intrathecal Drug Distribution: Key Factors for Interpatient Variability, *Anesthesia and Analgesia*, Vol. 115, 2012, pp. 879-879.

[71] Helgeland A, Mardal KA, Haughton V, Reif BA, Numerical Simulations of the Pulsating Flow of Cerebrospinal Fluid Flow in the Cervical Spinal Canal of a Chiari Patient, *Journal of Biomechanics*, VOl. 47, 2014, pp. 1082-1090

[72] Yiallourou TI, Kroger JR, Stergiopulos N, Maintz D, Martin BA, Bunck AC, Comparison of 4D Phase Contrast MRI Flow Measurements to Computational Fluid Dynamics Simulations of Cerebrospinal Fluid Motion in the Cervical Spine, *Plos One*, Vol.7, 2012, e52284.

[73] Sukumar, R., Ahavale, M.M., Makhijani, V.B., Przekwas, A.J, Application of Computational Fluid Dynamics Techniques to Blood Pumps, *Artificial Organs*, Vol.20, 1996, pp. 529–533.

[74] Chua, L.P., Song, G., Lim, T.M., Zhou, T, Numerical Analysis of the Inner Flow Field of a Biocentrifugal Blood Pump, *Artificial Organs*, Vol. 30, 2006, pp. 467–477.

[75] Katharine H. Fraser, M. Ertan Taskin, Bartley P. Griffith, Zhongjun J. Wu, The Use of Computational Fluid Dynamics in the Development of Ventricular Assist Devices, *Medical Engineering and Physics*, Vol. 33, No. 3, 2011, pp. 263–280.

[76] Farag MB, Karmonik C, Rengier F, Loebe M, Karck M, Von Tengg-Kobligk H, Ruhparwar A, Partovi S. Methodist Debakey, Review of Recent Results Using Computational Fluid Dynamics Simulations in Patients Receiving Mechanical Assist Devices for End-Stage Heart Failure, *Cardiovascular Journal*, Vol. 10, No. 3, 2014, pp. 185-9.

[77] Claudio Capelli, Chiara Corsini, Dario Biscarini, Francesco Ruffini, Francesco Migliavacca, Alfred Kocher, Guenther Laufer, Andrew M. Taylor, Silvia Schievano, Martin Andreas, Gaetano Burriesci, Claus Rath, Pledget-Armed Sutures Affect the Haemodynamic Performance of Biologic Aortic Valve Substitutes: A Preliminary Experimental and Computational Study, *Cardiovascular Engineering and Technology*, Vol. 8, No. 1, 2017, pp 17–29.